Molecular Recognition Effects in Metal Complex Mediated Double-Strand Cleavage of DNA: Reactivity and Binding Studies with Model Substrates

Charles A. Detmer III, Filomena V. Pamatong, and Jeffrey R. Bocarsly*

Department of Chemistry, The University of Connecticut, Storrs, Connecticut 06269

Received February 20, 1997[⊗]

Double-strand breaks in duplex DNA are thought to be significant sources of cell lethality because they appear to be less readily repaired by DNA repair mechanisms. We recently described the design and cleavage chemistry of ((2*S*,8*R*)-5-amino-2,8-dibenzyl-5-methyl-3,7-diazanonanedioato)copper(II) (**1**), which effects nonrandom double-strand cleavage of duplex DNA. After DNA nicking by generation of hydroxyl radicals, the key step in this process appears to occur through recognition by the metal complex of the nicked-abasic site on duplex DNA, followed by delivery of $OH^{\bullet}$ to cleave at the opposing strand, forming a double-strand lesion. Through the use of model nucleic acid substrates and comparison to DNA scission chemistry, we have investigated the electrostatic and hydrophobic contributions to DNA binding by complex **1**. We have complemented these reactivity studies with studies on the binding of **1** to a model nucleic acid substrate, using ^2H NMR spectroscopy with deuterated **1** and HDO T_1 relaxation enhancement methods to study the binding of **1** to nucleotide substrates. With these methods, we have estimated that the association constant for the $\mathbf{1}^{+}\cdot$5′-AMP^{2-} complex is $\sim$16 M^{-1} and that the binding interaction involves both electrostatic and aromatic stacking interactions between the nucleic acid base and the pendant aromatic side chains of **1**.

Introduction

Double-strand breaks (dsb's) in duplex DNA are thought to be more significant sources of cell lethality than are single-strand breaks (ssb's) because they appear to be less readily repaired by DNA repair mechanisms.[1,2] This insight makes the design of molecules that effect double-strand DNA cleavage an important goal from the perspective of drug design as well as that of the study of DNA repair mechanisms. We recently described the design and cleavage chemistry of a copper-based transition metal complex which performs nonrandom double-strand DNA cleavage.[3,4] This process appears to occur through recognition by the metal complex of an abasic-nicked site on duplex DNA.

Two classes of natural products have been shown to be active in mediating nonrandom double-strand DNA cleavage, the enediyne drugs[5] and the bleomycins.[6] The bleomycin drugs are paradigmatic for metal-mediated nonrandom double-strand DNA cleavage agents. As illustrated by bleomycin, a transition metal based double-strand cleavage agent must effect four events: nick formation on intact DNA, binding at the nicked site, reactivation, and complementary strand scission to form linear DNA. The design of a molecule which can perform these activities must therefore include a reactivatable metal center and recognition elements that bind both to duplex DNA and at abasic nick sites. Our initial complex ((2*S*,8*R*)-5-amino-2,8-dibenzyl-5-methyl-3,7-diazanonanedioato)copper(II) (**1**), employs phenylalanine side chains as hydrophobic recognition elements complemented by an ammonium group for electrostatic recognition of phosphate groups. The ammonium group is oriented below the coordination plane of the molecule, and the hydrophobic amino acid side chains are constrained to the opposite side of the coordination plane by the ligand framework. The rationale behind this molecular architecture is that the ammonium group can interact with phosphates on the DNA backbone, orienting the amino acid side chains toward the bottom of the groove, for interaction with the intact DNA groove or the hydrophobic DNA interior at accessible abasic nick sites. Copper(II) has been used extensively in metal-mediated DNA cleavage for the generation of hydrogen-abstracting activated oxygen species[7] and is also capable of DNA cleavage *via* phosphodiester hydrolysis.[8−10]

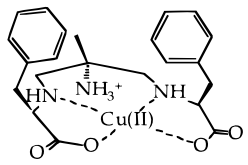

1

Our mechanistic studies of the double-strand cleavage activity of this copper complex have shown that **1** cleaves DNA through generation of a superoxide intermediate, via the production of hydroxyl radicals using the Haber−Weiss reaction.[4]

* To whom correspondence should be addressed.

[⊗] Abstract published in *Advance ACS Abstracts,* July 15, 1997.

(1) Povirk, L. F. In *Molecular Aspects of Anti-cancer Drug Action*; Neidle, S., Waring, M., Eds.; Verlag-Chemie: Weinheim, Germany, 1983; p 157.
(2) Povirk, L. F. *Mutat. Res.* **1991**, *257*, 127.
(3) Pamatong, F. V.; Detmer, C. A., III; Bocarsly, J. R. *J. Am. Chem. Soc.* **1996**, *118*, 5339.
(4) Detmer, C. A., III; Pamatong, F. V.; Bocarsly, J. R. *Inorg. Chem.* **1996**, *35*, 6292.
(5) Goldberg, I. H. In *Molecular Aspects of Anticancer Drug-DNA Interactions*; Neidle, S., Waring, M., Eds.; CRC Press: Boca Raton, FL, 1993; Vol. 1, p 243.
(6) Natrajan, A.; Hecht, S. M. In *Molecular Aspects of Anticancer Drug-DNA Interactions*; Neidle, S., Waring, M., Eds.; Press: Boca Raton, FL, 1993; Vol. 2, p 197.
(7) Barton, J. K. In *Bioinorganic Chemistry;* Bertini, I., Gray, H. B., Lippard, S. J., Valentine, J. S., Eds.; University Science Press: Mill Valley, CA, 1994; p 455.
(8) Kazakov, S. A. In *Bioorganic Chemistry: Nucleic Acids*; Hecht, S. M., Ed.; Oxford University Press: New York, 1996; p 244.
(9) Linkletter, B.; Chin, J. *Angew. Chem., Int. Ed. Engl.* **1995**, *34*, 472.
(10) Bashkin, J. K.; Frolova, E. I.; Sampath, U. *Am. Chem. Soc.* **1994**, *116*, 5981.

S0020-1669(97)00199-7 CCC: $14.00

Complex **1** appears to be capable of delivering $OH^{\bullet}$ to the intact DNA surface, to form a nicked abasic DNA site and subsequently to recognize and to bind the nicked abasic site for reactivation and cleavage at the opposing strand, forming a double-strand lesion in the DNA duplex. This sequence requires a number of recognition and binding events for double-strand cleavage to occur that presumably include both electrostatic and hydrophobic interactions. Through the use of simple model cleavage systems and their comparison to the DNA scission chemistry, we have attempted to investigate the electrostatic and hydrophobic contributions to DNA binding by complex **1**. We have complemented these reactivity studies with studies of the binding of **1** to a model nucleic acid substrate, using ^{2}H NMR spectroscopy of **1**-d_{10} and HDO T_1 relaxation enhancement methods to a study the binding of **1** to a nucleotide substrate.

Experimental Section

UV−vis spectra were recorded on an SLM-Aminco Milton-Roy 3000 diode array spectrophotometer, and fluorescence spectroscopy was performed on a Perkin-Elmer λ3 fluorescence spectrophotometer. pH and pD determinations were performed using a Fisher Scientific pH meter. GC-MS chromatography was performed using a Varian 3400 gas chromatograph−Finnegan MAT 700 system equipped with an ion-trap detector, and NMR experiments were performed on a Bruker 270 MHz NMR spectrophotometer or on a Bruker Avance DRX 400 NMR spectrophotometer. All materials were of reagent grade and were used without further purification unless otherwise noted. Calf thymus (CT) was purchased from Sigma and was purified using standard procedures.

DNA Scission Conditions. Electrophoresis experiments were performed with pUC18 DNA; all other experiments were done using calf thymus DNA. Scission reactions were performed at room temperature as follows. Reactions with pUC18 or CT DNA were performed using 10 μM DNA base pairs (bp's) and 100 μM metal complex in 20 mM phosphate buffer (pH 7.0) with activation by either 200 μM ascorbate/H_2O_2 or 1.0 mM H_2O_2. Reaction was quenched by addition of EDTA. Plasmid reaction products were separated by electrophoresis, and densitometric quantitation of electrophoresis gels was performed using a Macintosh Quadra 950 equipped with NIH Image software.[11] Supercoiled plasmid DNA values were corrected by a factor of 1.3, based on average literature estimates of lowered binding of ethidium to this structure.[12,13]

Hydroxyl Radical Assay by 2-Deoxy-D-ribose, Deoxyadenosine, or 5′-dAMP^{2-} Degradation. Hydroxyl radical production by **1** was assayed by degradation of a ribose-containing substrate, either 2-deoxy-D-ribose, deoxyadenosine (dA), or 5′-deoxyadenosine monophosphate (5′-dAMP^{2-}), followed by quantitation of the 2-thiobarbituric acid adduct.[14] A 100 μM sample of metal complex was reacted at room temperature with 1.0 mM ribose-containing substrate with activation by either 1.0 mM H_2O_2 or 190 μM H_2O_2 and sodium ascorbate. Reactions were performed in a 4 mL volume of 20 mM phosphate buffer (pH 7.0). Reaction solutions were quenched with EDTA (2.4 mM final concentration) and stored on ice. Each aliquot was then reacted with 2-thiobarbituric acid at 95 °C for 15 min. Workups were identical for all trials. The chromophore concentration was measured by fluorescence intensity at 553 nm (532 nm excitation). Fluorescence intensity was used because of its sensitivity and because of the fact that ascorbate byproducts absorb in the visible region, interfering with visible quantitation of the thiobarbituric acid adduct. Fluorescence intensity was converted to concentration with a standard fluorescence curve constructed using known concentrations of the chromophore, synthesized from malondialdehyde and 2-thiobarbituric acid.[15] Blank reactions lacking cleavage agent were included in each run, and the blank intensity was subtracted from each experimental point.

Hydroxyl Radical Assay by Rhodamine B Degradation. Hydroxyl radical production was quantitated using Rhodamine B[16] (6 μM) as the reporter molecule in the presence of 100 μM **1** with activation either by 1.0 mM H_2O_2 or by 190 μM each H_2O_2 and sodium ascorbate. Degradation of the dye was monitored at 552 nm ($\epsilon = 10.7 \times 10^4$ M^{-1} cm^{-1}). Reactions were performed in a 2.2 mL volume of 20 mM phosphate buffer (pH 7.0). Spectra of ~6 μM Rhodamine B with 100 μM **1** were identical to those of the dye in the absence of the metal complex, suggesting that Rhodamine B does not effectively coordinate to the metal center of **1** under the conditions used. Anaerobic runs were performed using a septum-equipped cuvette after purging with N_2.

Quantitation of Reduced 1, [1·Cu(I)], Formed during DNA Scission. The visible absorbance of **1** (100 μM) was monitored at 622 nm (thermostated cuvette at 25 °C) during the course of the reaction with CT DNA (10 μM bp) using sodium ascorbate/H_2O_2 tandem activation (190 μM each) or H_2O_2 activation (1.0 mM). The absorbance was converted to concentration using the measured extinction coefficient (85.3 M^{-1} cm^{-1}), and the measured values were subtracted from the initial concentration of **1** to obtain the amount of copper(I) complex formed.

^{2}H NMR Spectroscopy. ^{2}H NMR spectra were collected at 61.4 MHz in aqueous phosphate buffer (5 mM, pH 7.0) with a 0.6 s acquisition time using a 90° pulse (47 μs) with no lock at 23 °C in a standard 5 mm NMR tube. A total of 512 or 1024 transients were collected depending on the metal complex concentration. The spectra were referenced to the HDO peak, whose chemical shift was determined in relation to the DSS peak in the ^{1}H spectrum. Spectra were processed with 1.5 Hz line broadening and were then fit with Lorentzian functions to extract the chemical shifts of the components.

Estimation of the Binding Constant for 1 and 5′-AMP^{2-} by ^{2}H NMR Titration. The **1**−5′-AMP^{2-} binding constant was estimated by ^{2}H NMR titration of complex 1 deuterated at the aromatic positions. Complex **1** was synthesized using phenylalanine deuterated on the aromatic ring.[17] A 2.3 mM solution of **1**-d_{10} in 5 mM aqueous phosphate buffer (pH 7.0) was titrated with a stock solution of 5′-adenosine monophosphate (5′-AMP^{2-}) in a concentration range of 0−117 mM ribonucleotide. The initial pHs of both stock solutions were adjusted to identical values prior to titration in order to eliminate any pH-dependent shifts. ^{2}H NMR spectra were recorded at 23 °C as described above. Spectra were deconvoluted by Lorentzian curve fitting.

Estimation of the Binding Constant for 1 and 5′-AMP^{2-} by T_1 Measurements. Binding constants were estimated using the method of T_1 relaxation enhancement of the HDO peak of a solution containing paramagnetic metal ion and substrate.[18−20] T_1 values for solutions (5 mM deuterated phosphate buffer, pD 7.4) containing metal complex **1** (395 μM, constant for all determinations), substrate 5′-adenosine monophosphate (5′-AMP^{2-}) at varying concentrations up to 100 mM 5′-AMP^{2-}, or metal complex in the presence of substrate were measured using the standard inversion-recovery pulse sequence at 270 MHz (23

(11) The NIH Image program (written by Wayne Rasband at the U.S. National Institutes of Health and available from the Internet by anonymous ftp from zippy.nimh.nih.gov or on floppy disk from the NTIS, 5285 Port Royal Rd., Springfield, VA 22161, as part number PB93-504868) is public domain software.

(12) Hertzberg, R. P.; Dervan, P. B. *J. Am. Chem. Soc.* **1982**, *104*, 313.
(13) Mirabelli, C. K.; Huang, C.-H.; Crooke, S. T. *Cancer Res.* **1980**, *40*, 4173.
(14) Halliwell, B.; Gutteridge, J. M. C. In *CRC Handbook of Methods for Oxygen Radical Research*; Greenwald, R. A., Ed.; CRC Press: Boca Raton, FL, 1985; p 177.
(15) Burger, R. M.; Berkowitz, A. R.; Peisach, J.; Horwitz, S. B. *J. Biol. Chem.* **1980**, *255*, 11832.
(16) Farhataziz; Ross, A. B. *Selected Specific Rates of Reactions of Transients from Water in Aqueous Solution. III. Hydroxyl Radical and Perhydroxyl Radical and Their Radical Ions*; NSRDS-NBS 59; U.S. Department of Commerce/National Bureau of Standards: Washington, DC, 1977; p 59.
(17) Wishart, D. S.; Sykes, B. D.; Richards, F. M. *Biochim. Biophys. Acta* **1993**, *1164*, 36.
(18) Eisinger, J.; Shulman, R. G.; Blumberg, W. E. *Nature* **1961**, *192*, 963.
(19) Eisinger, J.; Shulman, R. G.; Szymanski, B. M. *J. Chem. Phys.* **1962**, *36*, 1721.
(20) Mildvan, A. S.; Cohn, M. *Biochemistry* **1963**, *2*, 910.

°C). For each determination, 15 τ values were chosen on the basis of an estimate of the null time. Data was analyzed using the integrated intensity of the HDO peak and were fit to the expression $f(\tau) = k[1 - 2\exp(-\tau/T_1)]$. Higher concentrations of 5′-AMP^{2-} were avoided to prevent complications associated with an increase in solution viscosity. Attempts to estimate a binding constant for dAMP^{2-} were unsuccessful because of the restricted solubility range of dAMP^{2-}.

NMR Data Analysis.[21] To account for the reduced level of free monomeric 5′-AMP^{2-} available for binding to **1**-d_{10} due to dimer formation, the following procedure was used. The NMR data (either chemical shift or T_1) were used to calculate the relevant experimental spectroscopic binding parameter. For chemical shift data, this is $\Delta = \delta_{obs} - \delta_{\mathbf{1}\text{-}d_{10}}$, where δ_{obs} is the chemical shift of the largest Lorentzian component of the aromatic peak packet during titration and $\delta_{\mathbf{1}\text{-}d_{10}}$ is the chemical shift of the largest Lorentzian component of the aromatic peak packet of free complex **1**-d_{10}. For T_1 data, the parameter is $\epsilon^* - 1$, where ϵ^* is the relaxation enhancement for the HDO peak due to the presence of paramagnetic complex:

$$\epsilon^* = \frac{\left(\frac{1}{T_1^*{}_{(M)}}\right) - \left(\frac{1}{T_1^*{}_{(0)}}\right)}{\left(\frac{1}{T_{1(M)}}\right) - \left(\frac{1}{T_{1(0)}}\right)} \quad (1)$$

$T_1^*{}_{(M)}$ is the HDO relaxation time in the presence of metal complex and biological ligand (5′-AMP^{2-}), $T_1^*{}_{(0)}$ is the HDO relaxation time in the presence of biological ligand and in the absence of metal complex, $T_{1(M)}$ is the HDO relaxation time in the presence of metal complex and in the absence of biological ligand, and $T_{1(0)}$ is the HDO relaxation time in the absence of metal complex and of biological ligand. Either of these experimental binding parameters P ($P = \Delta$ for chemical shift data and $\epsilon^* - 1$ for T_1 data) is fit to the 1:1 binding isotherm to extract the coefficients P_{11}:

$$P = \frac{P_{11}K_{assoc}[5'\text{-AMP}^{2-}]_{eq}}{1 + (K_{assoc}[5'\text{-AMP}^{2-}]_{eq})} \quad (2)$$

For chemical shift data, P_{11} is defined as $\Delta_{11} = \delta_{\mathbf{1}\cdot 5'\text{-AMP}} - \delta_{\mathbf{1}\text{-}d_{10}}$, where $\delta_{\mathbf{1}\cdot 5'\text{-AMP}}$ is the chemical shift for the largest Lorentzian component of the $\mathbf{1}^+\cdot$5′-AMP^{2-} complex. For T_1 HDO relaxation data, P_{11} is defined as $\epsilon_{11}^* - 1$, where ϵ_{11}^* is the HDO relaxation enhancement of the $\mathbf{1}^+\cdot$5′-AMP^{2-} complex. Using the total concentrations of 5′-AMP^{2-} as an initial estimate, the 1:1 binding isotherm was employed to estimate the values of the P_{11} parameters for each experiment. The estimated value of P_{11} was then used to recalculate $[5'\text{-AMP}^{2-}]_{eq}$, the equilibrium solution concentrations of monomeric 5′-AMP^{2-}, using the mass balance on 5′-AMP^{2-} and the 5′-AMP^{2-} dimer binding constant:

$$[5'\text{-AMP}^{2-}]_{tot} = [5'\text{-AMP}^{2-}]_{eq} + \left([\mathbf{1}]_{tot}\frac{P}{P_{11}}\right) + 2K_{dimer}([5'\text{-AMP}^{2-}]_{eq})^2 \quad (3)$$

K_{dimer} is estimated to be 1.8 M^{-1} at 23 °C from published data.[22] This process was iterated between estimates of P_{11} and $[5'\text{-AMP}^{2-}]_{eq}$ until the value of P_{11} changed by <0.01% between iterations; the converged P_{11} values from each of the experiments were used to generate estimates of K_{assoc} for the $\mathbf{1}^+\cdot$5′-AMP^{2-} complex by fits of the iterated values of $[5'\text{-AMP}^{2-}]_{eq}$ to eq 2.

Results

We previously showed that complex **1** effects nonrandom double-strand DNA cleavage[3] in the presence of reducing agent and hydrogen peroxide, through generation of hydroxyl radicals via the Haber−Weiss mechanism following eqs 4−7.[3,4] Dissociation of O_2^- (eq 6) may not be required for reaction, and reaction (eq 7) may be enhanced by the presence of the metal complex. Hydrogen peroxide may be added as an exogenous reactant, or it may be produced by dismutation of superoxide (eq 8). In investigating different cleavage activation systems for **1**, we noted that tandem activation with a reducing agent (sodium ascorbate) and hydrogen peroxide provides substantially greater levels of reactivity than does activation with higher levels of hydrogen peroxide alone. We have investigated the use of hydrogen peroxide as an activating agent for DNA cleavage by complex **1**, in order to try to evaluate whether cleavage chemistry of **1** at the macromolecular surface of DNA differs from the chemistry observed in solution. We have combined this study with an examination of the binding and cleavage chemistry of **1** with nucleic acid model substrates.

$$Cu^{II}(L) + e^- \rightarrow Cu^{I}(L) \quad (4)$$

$$Cu^{I}(L) + O_2 \leftrightarrows Cu^{II}(L)-O_2^- \quad (5)$$

$$Cu^{II}(L)-O_2^- \rightarrow Cu^{II}(L) + O_2^- \quad (6)$$

$$O_2^- + H_2O_2 \rightarrow O_2 + OH^- + OH^\bullet \quad (7)$$

$$O_2^- + O_2^- + 2H^+ \rightarrow O_2 + H_2O_2 \quad (8)$$

Mechanism of Cleavage Activation of 1 by Hydrogen Peroxide. To determine whether activation of **1** with a reducing agent (ascorbate) and H_2O_2 is mechanistically comparable to activation with H_2O_2 alone, we examined the latter system for evidence of a non-Haber−Weiss mechanism. We considered the possibility that activation of **1** by H_2O_2 alone could proceed through a competing mechanism, either the formation of a high-valent copper−oxo intermediate (described as a copper-bound hydroxyl radical[23]) or a Fenton mechanism. To evaluate the first alternate mechanism, reactivity studies between **1** with H_2O_2 and substrates known to react with high-valent metal−oxo species (*trans*-styrene, *cis*-styrene, and cyclohexene) were performed. None of the expected expoxidized products could be detected by GC-MS, using authentic products as standards (data not shown). This is inconsistent with a mechanism that proceeds through a metal−oxo intermediate (but does not rigorously eliminate a metal−oxo mechanism).

A competing mechanistic possibility is that activation of **1** with hydrogen peroxide proceeds through the production of diffusable hydroxyl radicals, by either a Haber−Weiss or a Fenton mechanism. We previously showed that lower levels of H_2O_2 (~200 μM H_2O_2 in the presence of exogenous reducing agent) activate **1** through the Haber−Weiss and not the Fenton pathway.[4] To clarify the mechanism of activation at higher levels of H_2O_2 (1.0 mM), we have examined whether H_2O_2 can serve as a reducing agent for **1** and whether any hydroxyl radicals can be detected when the reaction is performed under anaerobic conditions. As shown in Table 1, reduced **1** can be detected when H_2O_2 alone is used for activation of DNA cleavage; however, the levels are substantially lower than they are when ascorbate is included as reducing agent. Both sets of activation conditions produce a steady-state concentration of reduced **1** after an induction period of ~15 min (not shown). This verifies that H_2O_2 can serve as a reductant for **1**; however,

(21) Connors, K. A. *Binding Constants*; John Wiley & Sons: New York, 1987; Chapter 5.
(22) Egan, W. *J. Am. Chem. Soc.* **1976**, *98*, 4091.
(23) Kitajima, N.; Koda, T.; Iwata, Y.; Moro-oka, Y. *J. Am. Chem. Soc.* **1990**, *112*, 8833.

Table 1. Yields of [Cu^{I}(**1**)] and Hydroxyl Radicals during Cleavage by **1** (100 μM) as Functions of Cleavage Activation Conditions

activation conditions	product	quantitation	product concn[a]	ref
1.0 mM H_2O_2[b]	[Cu^{I}(**1**)]	[Cu^{II}(**1**)]	3 μM	this work
190 μM H_2O_2/ascorbate[b]	[Cu^{I}(**1**)]	[Cu^{II}(**1**)]	15 μM	4
1.0 mM H_2O_2 (anerobic)	$OH^{\bullet}$	Rhodamine B	13 nM	this work
1.0 mM H_2O_2[b]	$OH^{\bullet}$	Rhodamine B	160 nM	this work
1.0 mM H_2O_2[b]	$OH^{\bullet}$	2-deoxy-D-ribose	3 nM	this work
190 μM H_2O_2/ascorbate[b]	$OH^{\bullet}$	Rhodamine B	650 nM	4
190 μM H_2O_2/ascorbate[b]	$OH^{\bullet}$	2-deoxy-D-ribose	13 nM	4

[a] Steady-state concentration at 90 min of reaction. [b] Aerobic reaction.

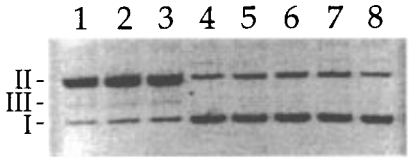

Figure 1. Agarose gel electrophoresis of cleavage of pUC18 DNA by **1** as a function of activation conditions. Metal complex concentrations: lanes 1 and 5, 50 μM **1**; lanes 2 and 6, 100 μM **1**; lanes 3 and 7, 150 μM **1**. Activation conditions: lanes 1−3, 200 μM H_2O_2/ascorbate; lanes 5−7, 1.0 mM H_2O_2. Lanes 4 and 8: DNA controls. Reaction conditions: 10 μM DNA bp pUC 18 in 20 mM phosphate buffer, pH 7.0. (Image is reversed for clarity.)

it does not distinguish between the Haber−Weiss and the Fenton pathways. Reaction of **1** and H_2O_2 with the hydroxyl radical trap Rhodamine B under anaerobic conditions allows differentiation between these two pathways, since the Fenton mechanism requires H_2O_2 and not dioxygen, while the Haber−Weiss mechanism requires both. As indicated in Table 1, anaerobic activation of **1** with H_2O_2 produces few trapped hydroxyl radicals, while identical aerobic activation produces ∼160 nM $OH^{\bullet}$. This suggests that a Haber−Weiss mechanism operates when **1** is activated by millimolar levels of H_2O_2 without an exogenous reducing agent. For comparison, the level of hydroxyl radicals produced by **1** on activation by H_2O_2 alone has been measured by reaction with 2-deoxy-D-ribose, a less efficient radical trap than Rhodamine B (in this system) but one that is chemically identical to the target moiety on the DNA substrate.

Study of the Effect of DNA Binding on Activation of 1 for Cleavage. The concentrations of $OH^{\bullet}$-mediated degradation events reported in Table 1 can be compared to the concentrations of DNA scission events quantitated by gel electrophoresis (Figure 1) under the same sets of reaction conditions. Quantitation of these DNA scission events, shown in Table 2, is based on the standard Poisson calculation of the average number of single-strand breaks (n_1) and double-strand breaks (n_2) per molecule in a plasmid DNA population.[24−26] As shown in Table 2, the ratio of strand scission events for activation by H_2O_2 alone vs H_2O_2/ascorbate is about 0.21 over a range of concentrations of complex **1**. The same ratio for hydroxyl radicals quantitated in free solution (Table 1) by both Rhodamine B and deoxyribose (at identical reaction times) is ∼0.25, values which are within experimental error of one another. This suggests that the fraction of complex **1** reduced and activated for cleavage chemistry in free solution is about the same as that formed on the DNA surface.

Molecular Recognition in Cleavage Chemistry. To examine more directly the effects of recognition events between complex **1** and substrate on the cleavage reaction, we have used model radical-trapping reactions with both uncharged deoxyadenosine and charged 5′-dAMP^{2-} as substrate radical traps. Figure 2 shows a comparison of radical trapping as a function of reaction time for these substrates, compared to the analogous levels previously determined for deoxyribose substrate.[4] The same steady-state curve is observed for all substrates. The negatively charged deoxyribonucleotide traps ∼26 nM radical at 90 min of reaction, while the uncharged deoxyribonucleoside traps about ∼16 nM radical, consistent with a significant role for the substrate−complex electrostatic interaction in the binding of **1** to a model substrate. The enhancement of deoxyribonucleoside cleavage over that of deoxyribose under identical conditions[4] (steady-state concentrations of ∼16 nM radical trapped by dA vs ∼13 nM radical trapped by deoxyribose) may indicate the presence of smaller contributions to binding from aromatic interactions between **1** and the nucleic acid base or from hydrogen-bonding interactions between the nucleoside and the metal complex.

Binding Studies of the Nucleotide·1 Complex. Enhanced $OH^{\bullet}$ trapping by a nucleotide should be reflected in the binding between the nucleotide and **1**. Since there are no shifts in the electronic spectroscopy of **1** upon interaction with nucleotides (or nucleosides) that can be used to monitor binding and the ^{1}H NMR method of complexation-induced chemical shifts is not readily applicable in the presence of a paramagnetic metal ion, the binding of a ribonucleotide to **1** was studied by alternate NMR techniques, ^{2}H NMR and HDO relaxation enhancement.

^{2}H NMR Binding Studies. ^{2}H NMR spectroscopy has been used with deuterated paramagnetic metal complexes for solution phase studies. It has been shown that deuterium NMR line widths in the presence of paramagnetic ions are substantially smaller than are the corresponding ^{1}H line widths.[27] The interaction between paramagnetic spins and deuterons does broaden ^{2}H lines; however, they are often sufficiently narrow for spectroscopic study. Accordingly, we have synthesized complex **1** with *d,l*-perdeuteriophenylalanine, *d,l*-phe-d_5, by substituting deuterated *d,l*-phe-d_5 for *d,l*-phe in the standard synthesis. The line width ratio between the aromatic peak envelope of **1**-d_{10} and that of free *d,l*-phe-d_5 in aqueous solution is ∼4. A typical ^{2}H NMR spectrum of **1**-d_{10} shows a single multiplet centered at δ ∼7.5 ppm, shown in Figure 3, with decomposition into Lorentzian components and residuals. All spectra of **1**-d_{10} proved to be fit adequately by three Lorentzian functions and a baseline correction function.

In order to examine the binding of complex **1** to 5′-AMP^{2-}, **1**-d_{10} was titrated with a stock solution of 5′-AMP^{2-} and the ^{2}H NMR spectrum was measured. Representative spectra from

(24) The fraction of linear DNA after scission chemistry is $f_{III} = n_2 \exp(-n_2)$. The fraction of supercoiled DNA remaining after treatment is $f_I = \exp[-(n_1 + n_2)]$.[25] The Freifelder−Trumbo relation is $n_2 = n_1^2(2h + 1)/4L$, where h is the maximum separation in base pairs between two cuts on complementary strands that produces a linear DNA molecule ($h = 16$) and L is the number of phosphoester bonds per DNA strand in the plasmid ($L = 2686$, [pUC18]).[26]

(25) Povirk, L. F.; Wubker, W.; Kohnlein, W.; Hutchinson, F. *Nucleic Acids Res.* **1977**, *4*, 3573.

(26) Freifelder, D.; Trumbo, B. *Biopolymers* **1969**, *7*, 681.

(27) Johnson, A.; Everett, G. W., Jr. *J. Am. Chem. Soc.* **1972**, *94*, 1419.

Table 2. Yields of DNA Strand Scission Events by **1** as a Function of Cleavage Activation Conditions

[**1**], μM	activation conditions	reaction time, min	n_1	n_2	total DNA scission events, nM	ratio[a]
50	1.0 mM H_2O_2	90	0.35		1.3	
50	190 μM H_2O_2/ascorbate	90	1.49	0.04	6.1	0.21
100	1.0 mM H_2O_2	90	0.34		1.3	
100	190 μM H_2O_2/ascorbate	90	1.54	0.04	6.2	0.21
150	1.0 mM H_2O_2	90	0.35		1.3	
150	190 μM H_2O_2/ascorbate	90	1.47	0.05	6.0	0.22

[a] Ratio of concentration of total DNA strand scission events under activation by 1.0 mM H_2O_2 to concentration of DNA strand scission events under activation by 190 μM H_2O_2/ascorbate.

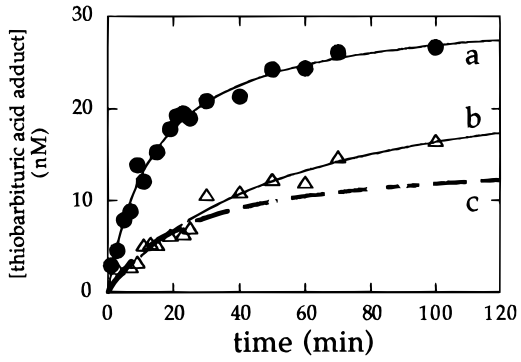

Figure 2. Quantification (by thiobarbituric acid adduct formation) of hydroxyl radical cleavage of (a) 5′-dAMP^{2-} (●) and (b) dA (△), with a comparison to (c) level of deoxyribose cleavage[4] (dashed curve) under identical conditions.

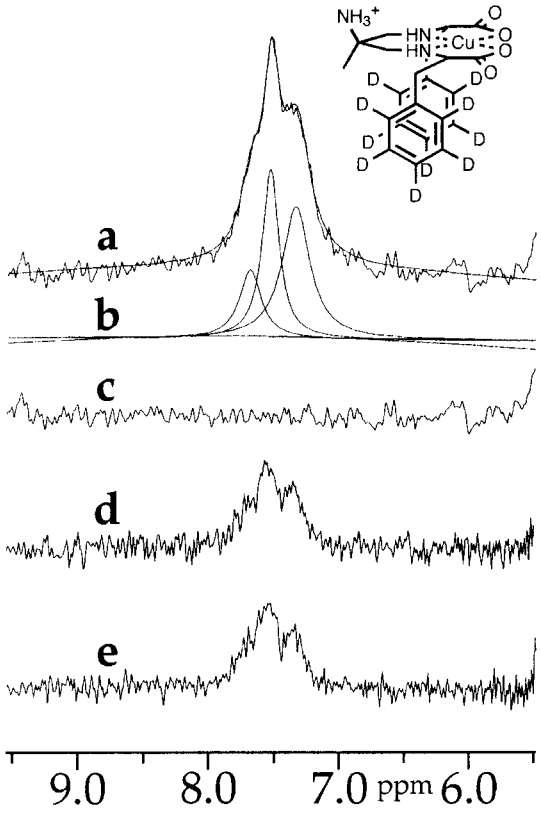

Figure 3. ^{2}H NMR spectra of complex **1**: (a) spectrum of **1** in 5 mM aqueous phosphate buffer (2.33 mM **1**) with Lorentzian fit; (b) Lorentzian fit components; (c) fit residual; (d) spectrum of **1** with 107 mM potassium sulfate added; (e) spectrum of **1** in 109 mM phosphate buffer.

the titration are shown in Figure 4. During the course of titration, the **1**-d_{10} signal maximum shifts by about 0.16 ppm upfield and the widths and intensities of the Lorentzian components of the peak packet change. Only a single peak envelope is observed during the titration, suggesting that the **1**$^+$•5′-AMP^{2-} complex exists under fast-exchange conditions.

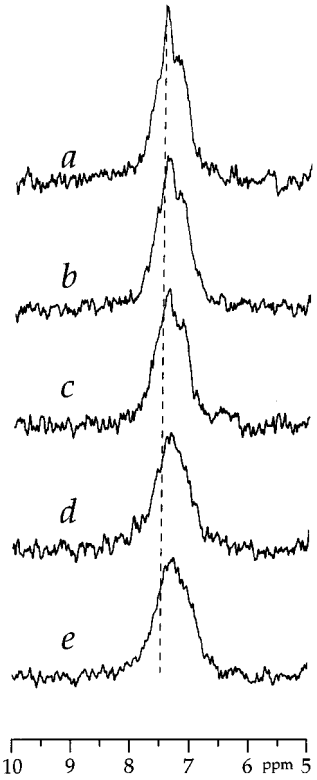

Figure 4. Selected ^{2}H NMR spectra of complex **1** (2.33 mM initial concentration) during titration with 5′-AMP^{2-} (5 mM aqueous phosphate buffer, pH 7): (a) 0 mM added 5′-AMP^{2-}; (b) 24.4 mM added 5′-AMP^{2-}; (c) 41.6 mM added 5′-AMP^{2-}; (d) 89.3 mM added 5′-AMP^{2-}; (e) 117 mM added 5′-AMP^{2-}. The dotted line marks the position of the peak maximum in the absence of titrant.

The changes in the spectra during the course of the titration are ascribed to binding between **1**-d_{10} and 5′-AMP^{2-}. Control spectra were taken to determine whether the observed effects could be due to phosphate coordination to the apical coordination site on the metal complex or to ionic strength changes during titration. Spectra of **1**-d_{10} with maximum limiting concentrations (>100 mM) of either phosphate buffer (to examine the possibility of phosphate coordination) or sulfate ion (an ion having the same charge as 5′-AMP^{2-}, but of low coordinating ability to **1**-d_{10}) were taken to check for spectral changes. Neither control spectrum showed any change compared to the spectrum of **1**-d_{10} (Figure 3d,e), confirming that the changes observed during titration with 5′-AMP^{2-} are due to formation of a **1**$^+$•5′-AMP^{2-} noncovalent complex.

Analysis of the titration of **1**-d_{10} by 5′-AMP^{2-} is complicated by the fact that 5′-AMP^{2-} forms dimers in aqueous solution.[22] The binding constant for the formation of the 5′-AMP^{2-} dimer at 23 °C can be interpolated from the published data[22] to be ~1.8 M^{-1}. The estimation of the **1**$^+$•5′-AMP^{2-} binding constant is performed by iterating between the values of the parameters of the 1:1 binding isotherm (eq 2) and the free solution

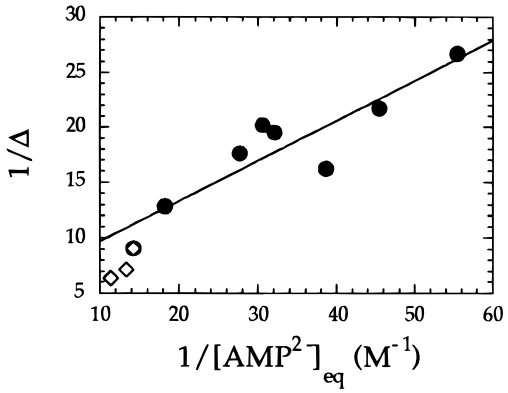

Figure 5. ^{2}H NMR binding study of the $\mathbf{1}^+$•5′-AMP^{2-} complex, with a least-squares fit (●) to the 1:1 binding isotherm (linear form of eq 2). ◇: points showing deviation from the low-concentration least-squares fit, ascribed to the presence of 5′-AMP^{2-} dimers.

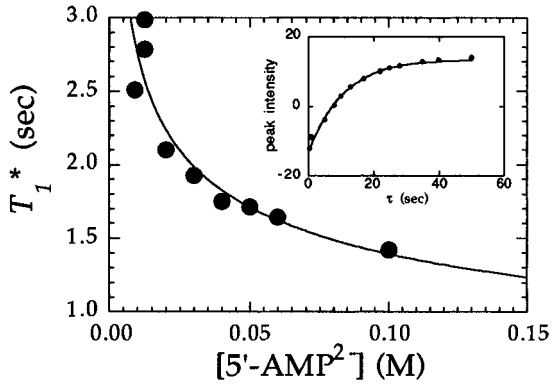

Figure 6. Dependence of T_1 of the HDO peak as a function of 5′-AMP^{2-} concentration in the presence of a constant concentration of **1** (395 μM). Inset: typical T_1 determination for the HDO peak (395 μM **1**, 50 mM 5′-AMP^{2-} concentration).

concentration of 5′-AMP^{2-} at equilibrium, using an expression for the mass balance of 5′-AMP^{2-} (eq 3; see Experimental Section for details). Figure 5 shows the titration results, graphed according to the linear form of eq 2. At higher concentrations of 5′-AMP^{2-}, the curve appears to depart from linearity, suggesting that a simple 1:1 binding assumption is no longer appropriate for this concentration regime. Studies of 5′-AMP^{2-} dimerization have indicated that association beyond the dimer stage occurs.[22] We therefore excluded the highest concentration points from the fit, leading to a binding constant estimate from these data of $K_{assoc} = 16.6$ M^{-1}.

***T*$_1$ HDO Binding Studies.** A parallel estimate of the association constant for the $\mathbf{1}^+$•5′-AMP^{2-} complex was undertaken using the strategy of T_1 relaxation enhancement of the HDO peak. Relaxation enhancement of water protons is a short-range effect (r^{-6} dependence) that is observed when rapidly-relaxing water protons in the hydration sphere of the paramagnetic metal complex are in fast exchange with bulk water. Binding of the metal complex to biological ligands can lead to an increase in the correlation time of the complex, which results in an enhancement in relaxation.[18−20] The T_1 values for the HDO peak of solutions containing a constant concentration of paramagnetic metal complex **1** (395 μM) and varying concentrations of 5′-AMP^{2-} were measured using the standard inversion-recovery pulse sequence. Figure 6 shows that the expected reduction in the T_1 values of the HDO peak does occur as the 5′-AMP^{2-} concentration is raised.

From these data, with parallel determinations for solutions of the ribonucleotide without the metal complex, the relaxation enhancement ϵ^* is calculated (eq 1). The dependence of the relaxation enhancement parameter for the 1:1 binding isotherm, ($\epsilon^* - 1$), on the concentration of 5′-AMP^{2-} in the presence of **1** is shown in Figure 7. The same iterative procedure as described for the ^{2}H NMR experiment above was employed to include the effects of 5′-AMP^{2-} dimerization. Higher concentration peaks that departed substantially from the 1:1 binding isotherm were likewise not included. A value of $K_{assoc} = 16.4$ M^{-1} is estimated from these data, in reasonable agreement with the value determined by ^{2}H NMR titration.

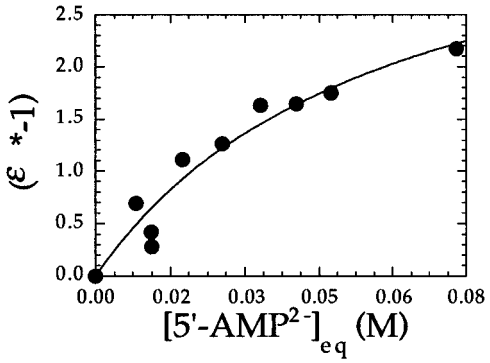

Figure 7. Relaxation enhancement binding study of the $\mathbf{1}^+$•5′-AMP^{2-} complex, with a nonlinear least-squares fit to the 1:1 binding isotherm (eq 2).

Discussion

The comparison of cleavage events quantitated using both sets of activation conditions can be used to clarify some of the characteristics of binding of **1** to DNA. The ratio of trapped radicals quantitated using 1.0 mM H_2O_2 activation to trapped radicals quantitated using tandem ascorbate/H_2O_2 (200 μM each) activation in free solution is roughly equal to the same ratio found for DNA cleavage (Table 2). Assuming that the solution quantitations are roughly proportional to the actual number of radicals formed (which is not rigorously true because the hydroxyl radical quantitations do not account for radicals that interact with species other than the traps), this comparison suggests that the fraction of activated, OH•-generating complex **1** bound to DNA is about the same as that found in free solution. Therefore, it appears that reduction of **1** during the activation cycle does not dramatically affect its on-rate to the DNA surface relative to the rate of scission chemistry. If this were the case, then the ratio should be lower for the DNA cleavage chemistry than for the free solution radical-trapping chemistry, since tandem H_2O_2/ascorbate activation produces higher levels of reduced **1** than activation by H_2O_2 alone, which would lead to greater binding and reactivity and a lower ratio. Likewise, this result appears to suggest that reduction of DNA surface-bound **1** does not dramatically enhance the off-rate of bound **1** relative to the chemical steps, since, by a similar argument, this should cause the ratio to be significantly higher for reaction in free solution than for reaction at the DNA surface. This picture is consistent with one in which binding to the DNA surface is the rate-limiting step in the cleavage cycle, leading to a situation where the fraction of cleavage-activated complex on the DNA surface is about the same as that found in free solution.

The contributions to binding of **1** to DNA may be assessed from the model cleavage reactions and NMR studies described above. The comparison of cleavage events quantitated with ribose, ribonucleoside dA, and 5′-dAMP^{2-} suggests that each model substrate has a different binding affinity for complex **1**, since the chemical steps involved in radical trapping and quantitation by the 2-deoxy-D-ribose moiety of each should be identical. We attribute the difference in trapping efficiency

between the charged substrate, 5′-dAMP^{2-}, and the neutral dA or 2-deoxy-D-ribose to the difference in binding interactions between these substrates and **1**. The two possible dominant interactions between **1** and 5′-dAMP^{2-} are (i) electrostatic interactions between the charge of the ammonium group of **1** and that of the substrate phosphate and (ii) a coordination interaction of the nucleotide phosphate at the axial site on the metal complex. We rule out the latter possibility on the basis of the absence of an observable spectroscopic response of the copper chromophore of **1** to the presence of the nucleotide. This is supported by the ^{2}H NMR spectra, in which a response is observed for the ribonucleotide but not for the phosphate ion. Finally, there is only one available axial coordination site on complex **1**, since the phenylalanine side chains tend to sterically block the opposite face; this site is required for coordination events related to hydroxyl radical production. If this site were blocked by phosphate coordination, reactivity would be expected to be depressed and not enhanced in 5′-dAMP^{2-} vs dA.

The difference in degradation between dA and 2-deoxy-D-ribose, which differ structurally only by the presence of the nucleic acid base, is significant, since it points to an additional interaction beyond the observed electrostatic interaction. Candidates for this interaction are the potential coordination of N7 of adenine to the copper center, a hydrogen-bonding interaction between the base and the metal complex, dipole−dipole interactions, and a hydrophobic interaction between the adenine base and the phenylalanine side chains of the complex. We can rule out the possibility of adenine coordination on the same grounds as phosphate coordination was excluded above: there is no observable spectroscopic response of the copper chromophore to the presence of the dA (data not shown), and reactivity with dA should be suppressed, not enhanced, compared to reactivity with deoxyribose if the base coordinates. A hydrogen-bonding interaction between the nucleotide base and groups on the metal complex, a dipole interaction, or a hydrophobic stacking interaction between pendant phenylalanine side chains of **1** and the nucleoside base a cannot be excluded on the basis of the electronic spectroscopy of the complex.

The possibility of the last interaction, a hydrophobic or aromatic stacking interaction between the benzene rings of **1** and the substrate base, is supported by the ^{2}H NMR data. The direction of the chemical shift change in the aromatic ^{2}H resonances should respond to interactions with an aromatic π-system as do resonances of other nuclei.[28] The upfield ^{2}H shift is consistent with similar shifts observed in the ^{1}H NMR of DNA-intercalated planar aromatic groups.[28] For protons, the size of the chemical shift change ranges from 0.4 to 1 ppm, on going from a weak DNA intercalator to a strong intercalator.[29] The change observed in our system is a modest ∼0.2 ppm, the size of which may be due to the difference in the stacking efficiencies of free nucleotides vs intact DNA with the side chains of **1**, or it may reflect differences between protons and deuterons in spectroscopic response to the aromatic interaction.

The NMR binding studies presented above independently confirm that weak binding occurs in the **1**$^+$·5′-AMP^{2-} complex, with $K_{assoc} \sim 16$ M^{-1}. Aromatic stacking interactions similar to those proposed here have been extensively studied by Sigel and co-workers,[30,31] including measurement of the association constants for complexation between different adenosine phosphates and planar aromatic heterocycles (2,2′-bipyridyl or 1,10-phenanthroline). K_{assoc} for these systems was determined to be between 16 and 38 M^{-1}.[32] Binding constant estimations based on oxidative chemistry between [Ru(terpy)(bpy)O]$^{2+}$ and nucleotides have been made by Thorpe and co-workers, with values in the range 15−48 M^{-1}.[33] Our experimental values fall at the low end of these ranges. The aromatic heterocycle−adenosine phosphate interactions studied by Sigel have no electrostatic component as does the **1**$^+$·5′-AMP^{2-} complex, yet the binding in the **1**$^+$·5′-AMP^{2-} complex is generally weaker. The explanation may be related to the observation that K_{assoc} for the aromatic heterocycle−adenosine phosphate systems is known to be dependent on the amount of planar aromatic surface area involved in the interaction.[32] A smaller stacking interaction is expected in the **1**$^+$·5′-AMP^{2-} complex because the phenylalanine side chains provide less aromatic surface area than do the aromatic heterocycles studied by Sigel or Thorp. This suggests that the sum of the electrostatic and the relatively small aromatic stacking contributions in the **1**$^+$·5′-AMP^{2-} complex may bring the total binding interaction in the **1**$^+$·5′-AMP^{2-} complex into the range of the interactions studied by Sigel.

The notion that phenylalanine side chains can participate effectively in aromatic stacking has literature precedent from studies of nonnatural DNA nucleotides and from studies of protein−DNA interfaces. Nonnatural DNA nucleotides containing benzene rings as bases have been shown to have aromatic stacking affinities in DNA competitive with the stacking affinities of DNA bases (the benzene ring has a stacking affinity between those of thymine and adenine).[34] In addition, stacking interactions between phenylalanine (among other aromatic amino acids) and nucleic acid bases have been observed at protein−DNA interfaces in crystal structures of DNA-binding proteins.[35]

These observations, taken with the data presented in the study, suggest that the modes of molecular recognition utilized by complex **1** in effecting double-strand cleavage of duplex DNA include stacking interactions between a pendant phenylalanine ring of **1** and DNA bases and electrostatic interactions. If, as seems likely, there is a greater range of electrostatic, hydrophobic, and hydrogen-bonding interactions available to **1** bound at abasic nicked sites on DNA than there is in the **1**$^+$·5′-AMP^{2-} complex, then binding constants higher than those reported here are to be expected for binding of **1** to DNA. Previously,[3,4] we have suggested that the double-strand cleavage cycle of **1** starts with the binding of **1** at the intact surface of duplex DNA, with activation and formation of an abasic nick site. Complex **1** recognizes this site and can bind through a combination of electrostatic and hydrophobic interactions for reactivation of scission chemistry and cleavage at the complementary strand. The binding interactions characterized in this study with model substrates confirm that **1** is competent to engage in these types of interactions with a nucleic acid substrate. Studies are continuing to determine whether these interactions can be characterized by similar methods with a DNA substrate.

Acknowledgment. We wish to acknowledge helpful discussions with Prof. C. V. Kumar.

IC970199P

(28) Giessner-Prettre, C.; Pullman, B. *Q. Rev. Biophys.* **1987**, *20*, 113.
(29) Wilson, W. D.; Strekowski, L.; Tanious, F. A.; Watson, R. A.; Mokrosz, J. L.; Strekowska, A.; Webster, G. D.; Neidle, S. *J. Am. Chem. Soc.* **1988**, *110*, 8292.
(30) Martin, R. B.; Sigel, H. *Comments Inorg. Chem.* **1988**, *6*, 285.
(31) Sigel, H. *Pure Appl. Chem.* **1989**, *61*, 923.
(32) Massoud, S. S.; Tribolet, R.; Sigel, H. *Eur. J. Biochem.* **1990**, *187*, 387.
(33) Neyhart, G. A.; Cheng, C.-C.; Thorp, H. H. *J. Am. Chem. Soc.* **1995**, *117*, 1463.
(34) Guckian, K. M.; Schweitzer, B. A.; Ren, R. X.-F.; Sheils, C. J.; Paris, P. L.; Tahmassebi, D. C.; Kool, E. T. *J. Am. Chem. Soc.* **1996**, *118*, 8182.
(35) Werner, M.; Gronenborn, A. M.; Clore, G. M. *Science* **1996**, *271*, 778.